EUROFUSION CP(15)03/12

P. Dumortier et al.

Calibrations and Verifications Performed in View of the ILA Reinstatement at JET

(27th April 2015 – 29th April 2015)
Lake Arrowhead, California, USA

This work has been carried out within the framework of the EUROfusion Consortium and has received funding from the Euratom research and training programme 2014-2018 under grant agreement No 633053. The views and opinions expressed herein do not necessarily reflect those of the European Commission.

Calibrations and Verifications Performed in View of the ILA Reinstatement at JET

P. Dumortier[1,a)], F. Durodié[1], W. Helou[2], I. Monakhov[3], C. Noble[3], E. Wooldridge[3], T. Blackman[3], M. Graham[3] and JET Contributors[*]

EUROfusion Consortium, JET, Culham Science Centre, Abingdon, OX14 3DB, UK

[1]*LPP-ERM-KMS, TEC partner, Brussels, Belgium*
[2]*CEA, IRFM, F-13108 St-Paul-Lez-Durance, France*
[3]*CCFE, Culham Science Centre, Abingdon, United Kingdom*

[a)]Corresponding author: pierre.dumortier@rma.ac.be

Abstract. The calibrations and verifications that are performed in preparation of the ITER-Like antenna (ILA) reinstatement at JET are reviewed. A brief reminder of the ILA system layout is given. The different calibration methods and results are then discussed. They encompass the calibrations of the directional couplers present in the system, the determination of the relation between the capacitor position readings and the capacitance value, the voltage probes calibration inside the antenna housing, the RF cables characterization and the acquisition electronics circuit calibration. Earlier experience with the ILA has shown that accurate calibrations are essential for the control of the full ILA close-packed antenna array, its protection through the S-Matrix Arc Detection and the new second stage matching algorithm to be implemented. Finally the voltage stand-off of the capacitors is checked and the phase range achievable with the system is verified. The system layout is modified as to allow dipole operation over the whole operating frequency range when operating with the 3dB combiner-splitters.

INTRODUCTION

The ITER-like Antenna (ILA) installed on JET is composed of four resonant double loops (RDLs) arranged in a 2 toroidal by 2 poloidal array. Each RDL consists of two poloidally adjacent straps fed through in-vessel matching capacitors from a common Vacuum Transmission Line (VTL) [1,2]. The capacitors are adjusted such that the impedance at the conjugate-T junction matches a chosen impedance Z_{CT} (real part: *3…10Ω*, imaginary part: *-2…0 Ω* to compensate for mutual coupling effects between the RDL straps). A quarter-wave (at *42.5MHz*) impedance transformer (the *9Ω* characteristic impedance VTL) and a second matching stage (stub + phase shifter) transform Z_{CT} into the Main Transmission Line (MTL) characteristic impedance (*30Ω*). Two toroidally adjacent RDLs are fed from a 3dB-hybrid splitter, by *4MW* coming from combining two *2MW* RF sources through a 3dB-hybrid combiner. The phase between two toroidally adjacent RDLs fed by the same hybrid splitter is adjusted by phase shifters in the MTL. The ILA operates from *29* to *47* (possibly *49*) *MHz* [3].

CALIBRATION PROCEDURES

Earlier experience has shown that accurate calibration is essential for the control of the full ILA close-packed antenna array as well as for the protection of the antenna through the S-Matrix Arc Detection (SMAD) [4]. It is also essential for the new second stage matching algorithm that is being implemented [3].

[*] See the Appendix of F. Romanelli et al., Proceedings of the 25th IAEA Fusion Energy Conference 2014, Saint Petersburg, Russia.

Directional Couplers Calibration

The calibration of the directional couplers in the different lines of the system is performed in-line and requires the characterization of the *9* inches *30Ω* (and *6* inches *30Ω*) to type-N *50Ω* RF adaptors, which are used to perform the network analyzer measurements. As no *9"* (or *6"*) - *30Ω* calibration standard is available an ad-hoc technique has to be used. Two techniques are considered: Two-Lines and Line+Open. In the first S-matrix measurements are performed on two sections of lines of different lengths with a similar measurement adaptor on both ends. In the second one S-matrix measurements are performed on one section of line with a measurement adaptor on both ends and on one section of open line with a measurement adaptor on one end (reflection measurement). Following assumptions are made: all measurement adaptors are similar, circuits are reciprocal, electrical lengths of the lines are precisely known and lines are lossless. In the case of the open line measurement a numerical model of the line is used to estimate the stray capacitance at the open end.

Both methods are sensitive to noise. Figure 1a shows an example of $|S_{11}|$ extracted using the two methods when numerically introducing some measurement noise to the adaptor S-matrix components. It is seen that the Line+Open method is less sensitive to noise than the Two-Lines method. One can also note that the accuracy is lost for specific frequencies, which are function of the chosen lengths for the line sections.

The scattering matrix components of the measurement adaptor with the Line+Open method are the following:

$$\begin{aligned} S_{11} &= \frac{\Gamma\left(L_{11}^2 - L_{12}^2\right) + G\left(L_{12}\, e^{j\beta(2n-l)} - \Gamma L_{11}\right)}{\Gamma\left(L_{11} - G\right) + L_{12}\, e^{j\beta(2n-l)}} \\ S_{22} &= \frac{\left(L_{11} - G\right)e^{2j\beta n} + \Gamma L_{12} e^{j\beta l}}{\Gamma\left(L_{11} - G\right) + L_{12}\, e^{j\beta(2n-l)}} \\ S_{12}S_{21} &= S_{12}^2 = L_{12}\left(e^{j\beta l} - e^{-j\beta l} S_{22}^2\right) \end{aligned} \tag{1}$$

where $\beta=2\pi f/c$ is the propagation constant, $\Gamma = \left(1 - j\omega C Z_0\right)/\left(1 + j\omega C Z_0\right)$ is the open-end reflection coefficient, C is the stray capacitance at the open–end and Z_0 is the line characteristic impedance. $[L]$ is the S-matrix of the Line (or thru) measurement of the section of line of length l and G is the reflection measurement of the Open line of length n.

The lengths l and n need to be adequately chosen as the denominators of S_{11} and S_{22} go to zero leading to a loss of accuracy for frequencies equal to:

$$f = \frac{k\, c}{2\left|l - 2n\right|}, \quad k = 0,1,2,... \tag{2}$$

The directional couplers are calibrated in-line (see Fig. 1b), meaning that the section of line containing the directional couplers is isolated and fitted with measurement adaptors on both ends. The calibration coefficients are then obtained by de-embedding the measurement adaptors from the 4-port S-matrix measurement of the line section and directional couplers and by shifting the excitation signals to the directional couplers plane. The S-matrix components of interest are the coupling and directivity terms.

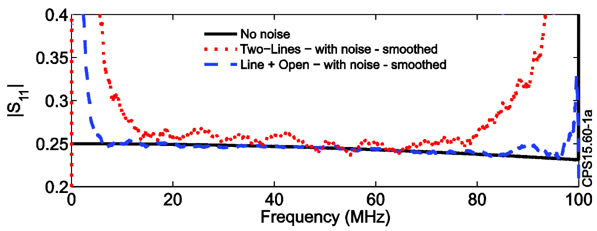

(a)

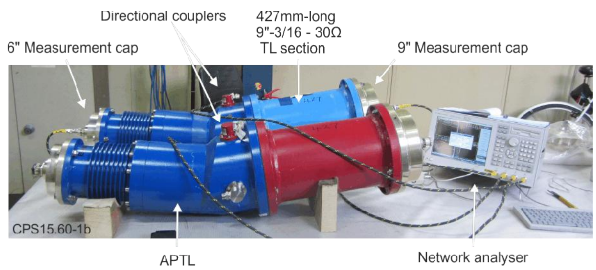

(b)

FIGURE 1. (a) Magnitude of the S_{11} component in ideal or no noise case (plain) and obtained by Two-Lines (dotted) and Line+Open (dashed) methods with noisy signals (b) Experimental set-up for the calibration of the APTL directional couplers.

Capacitor Calibration

The linear relationship between the capacitors' position potentiometer readings and the DC capacitance is established for each of the 8 ILA capacitors prior to the installation of the VTLs on JET. This information will be used to bring the capacitors to their initial value as well as in the RF modelling of the ILA circuit. A dedicated LabView code was developed in order to actuate the capacitors acting on the hydraulics and record the readings of the capacitance (measured by an LCR-meter) and position potentiometers. Special attention needed to be brought to avoid ground loops perturbing the capacitance measurements. It was verified that all potentiometers are operational and that all capacitors achieve the required *80-300pF* capacitance range.

Capacitor Voltage Probes Calibration

The voltages in the ILA are monitored by 16 voltage probes located at the vacuum matching capacitors (2 per capacitor/strap). These RF probe signals are used for antenna protection (voltage limit, SMAD), to control the phases of the strap currents and to assess the quality of the voltage balance across the array.

The in-situ amplitude and phase calibration of the voltage probes is carried out using a dummy capacitor mounted on a dedicated mechanical system and inserted inside the VTL. Figure 2a shows a cut view of the set-up and Fig. 2b displays the electrical schematic of the circuit. The voltage probe acts as a capacitive voltage divider. In first instance the capacitance C_{1v} between the voltage probe tip and the variable electrode can be neglected as the voltage at the variable electrode is about *10%* of the voltage at the fixed electrode and C_{1v} was moreover shown to be about *10%* of the capacitance between the voltage probe tip and the fixed electrode C_{1f}. The ratio $k_{V,pr}$ between the voltage at the fixed electrode (at probe location, V_C) and the voltage measured at the probe tip (V_{pr}) is given by :

$$k_{V,pr} = \frac{V_C}{V_{pr}} \approx \frac{1 + j\omega(C_{1f} + C_2)Z_{pr}}{j\omega C_{1f} Z_{pr}} = \frac{1}{j\omega C_{1f} Z_{pr}} \quad if \quad \omega(C_{1f} + C_2)\left|Z_{pr}\right| << 1 \tag{3}$$

Numerical simulations have shown that the coefficient $k_{V,pr}$ is almost independent of the loading of the strap. Typical values are $C_{1f}=54fF$, $C_2=1.6pF$, $\omega=2\pi f=O(3\ 10^8\ s^{-1})$, $Z_{pr}=50\Omega$ and hence $\omega(C_{1f}+C_2)|Z_{pr}|\approx 0.025<<1$. The amplitude of $k_{V,pr}$ is decreasing as $1/f$ (i.e. *20dB/decade*) and its phase is close to $-\pi/2$.

The calibration is done as in [5] by exciting the fixed electrode of the dummy capacitor and measuring the probe signal while the variable electrode is grounded by a short circuit flange (see Fig. 2a). The measurement is performed at the junction box and the calibration also accounts for the cabling (Thermocoax + RF jumper cable) up to the junction box. The measurement gives the ratio of the voltage measured at the junction box to the excitation signal: $k_{Vm}=V_m/V_{exc}$. A numerical model of the RF circuit (dummy capacitor, voltage probe, antenna housing) is needed to relate the voltage at the probe location to the excitation signal, $k_{VC}=V_C/V_{exc}$. This serves as a reference to calibrate the measured signal. The resulting calibration coefficient is finally given by $k_V=V_C/V_m=k_{VC}/k_{Vm}$.

Figure 2c shows an example of the magnitude of the coefficient obtained by the calibration, which is as expected from Eq. 3 decreasing in *1/f*. The ripple is due to slight impedance mismatch of the Thermocoax probe cable and is taken into account in the calibration. Attenuation and electrical length of the probe cable are taken into account in k_V.

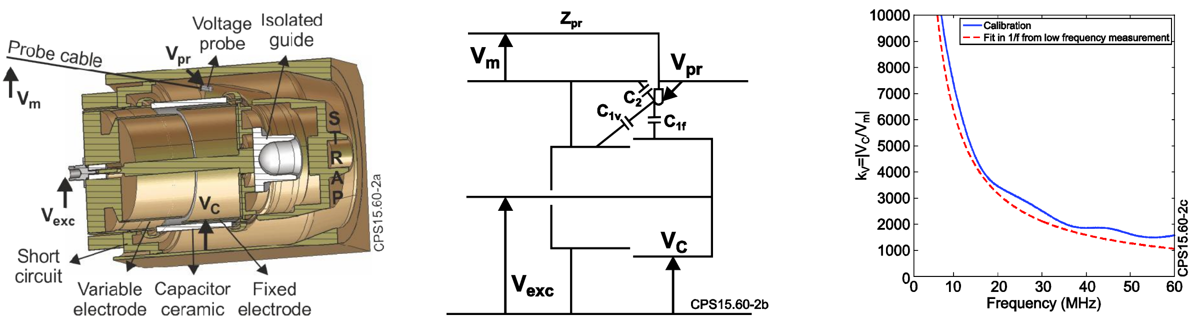

(a) (b) (c)

FIGURE 2. (a) Cut view of the experimental set-up for voltage probe calibration (b) Electrical circuit (c) Example of calibration curve extracted from the combination of measurements and numerical simulations.

RF Cables Calibration

All RF cables (up to *80m* length) fitted with possible elbows and adapters are calibrated before connection to the measurement connector (directional couplers, voltage probes). Electrical length and attenuation are obtained from a reflection measurement on the cables with open or short-circuited end.

Electronics Calibration

All RF signals are down-converted to a fixed Intermediate Frequency (IF) $f_{IF} = 1.3MHz$ by a RF Conversion Module (RFCM). The RFCM contains a mix-mod board that converts and filters an input RF signal down to the IF and outputs a signal for demodulation by the Amplitude and Phase Detection Module (APDM). This module splits the incoming IF signal in two and mixes the outputs with local phase reference signals *90°* apart. The in-phase and quadrature signals are filtered and sampled. The digital signal can then be processed to obtain the amplitude and phase of the RF signals.

A reference signal of amplitude V_{in} (*0-10dBm*) is generated at frequency f_k+IF, where f_k is an operating frequency (*29-49MHz*). This signal is split and injected into the RFCM inputs of a reference channel and of a measurement channel. The splitting network is characterized by a network analyzer measurement. The RFCM down-converts the signals to a frequency $IF+\varepsilon$, where $\varepsilon=O(Hz)$ is used to provide a phase sweep. Scan of frequency and amplitude and recording of the amplitude and phase outputs are automatically controlled by a LabView software running on the ILA PXI control crate.

Finally a global calibration coefficient to be applied to each individual measurement is determined by combining the calibrations of all the elements of the measurement chain.

OPERATIONAL VERIFICATIONS

High voltage testing of the capacitors prior to their installation on the machine revealed that capacitor C7 didn't meet the stand-off requirements (*2* minutes at *48kV* DC). The voltage stand-off degradation is attributed to the degraded vacuum conditions inside the capacitor resulting from the storage over many years of the capacitor without use. Conditioning pulses were applied. The voltage stand-off could be recovered and the requirement met.

Two toroidal RDLs (upper or lower) are fed through one 3dB-hybrid splitter. The phase difference between the currents in the two branches at the output of the hybrid splitter is $\pi/2$. One consequently needs to adjust the length of the trombones in the MTLs in order to provide the dipole phasing required by the physics program for heating over the whole range of operating frequencies, i.e. at least from *29MHz* to *49MHz*. A 3-port S-matrix measurement is performed with port 1 connected to the 3dB-hybrid splitter input and ports 2 and 3 connected on the MTLs at the level of the second stage matching stubs. The phase difference across the operational frequency range is then determined. A first measurement allowed identifying the necessary changes in the MTL lengths to ensure operation in dipole phasing for all operating frequencies. Changes were implemented and it was verified that operation in toroidal dipole phasing (and co-current drive phasing) was possible for all operating frequencies.

ACKNOWLEDGMENTS

This work has been carried out within the framework of the EUROfusion Consortium and has received funding from the Euratom research and training programme 2014-2018 under grant agreement No 633053. The views and opinions expressed herein do not necessarily reflect those of the European Commission.

REFERENCES

1. F. Durodié et al., AIP Conf. Proc. **595** (2001) 122-125.
2. F. Durodié et al., Fusion Engineering and Design **84** (2009) 279–283.
3. F. Durodié et al., this conference.
4. M. Vrancken et al., Fusion Engineering and Design **84** (2009) 1953–1960.
5. M. Vrancken et al., Fusion Engineering and Design **82** (2007) 873–880.